Korean J. Chem. Eng., 38(6), 1170-1178 (2021)
DOI: 10.1007/s11814-021-0768-6

pISSN: 0256-1115
eISSN: 1975-7220

Application of 2-methylfuran and 5-methylfurfural for the synthesis of C16 fuel precursor over fibrous silica-supported heteropoly acid-functionalized ionic liquid

Mahlet Nigus Gebresillase*,‡, Reibelle Quiambao Raguindin,‡, and Jeong Gil Seo*,†**

*Department of Chemical Engineering, Hanyang University, 222 Wangsimni-ro, Seongdong-gu, Seoul 04763, Korea
**Department of Energy Science and Technology, Myongji University,
116 Myongji-ro, Cheoin-gu, Yongin-si, Gyeonggi-do 17058, Korea
(*Received 14 November 2020 • Revised 15 February 2021 • Accepted 23 February 2021*)

Abstract−Lignocellulosic biomass is the most abundant renewable and sustainable carbon source with great potential for the synthesis of biofuels. In this study fibrous nano-silica (FNS) supported heteropoly acid-functionalized ionic liquid (FNS-ILHPW) catalyst was synthesized for the cross-condensation reaction of 2-MF and 5-MF to produce C16 fuel precursor. 2-MF and 5-MF were utilized in a stoichiometric ratio. The prepared catalysts were characterized by scanning electron microscopy (SEM), Fourier transform infrared spectroscopy (FT-IR), X-ray diffraction (XRD), and thermal gravimetric analysis (TGA). The obtained result from the XRD and FTIR suggests that HPW was present as charge compensating anion ($H_2PW_{12}O_{40}^-$) of the IL. NH_3-TPD analysis revealed that FNS-ILHPW retains moderate to strong acid sites. FNS-ILHPW shows higher conversion of the reactants and selectivity to C16 (2, 2′,2″-methylidenetris[5-methylfuran]) fuel precursor. 95% yield of C16 fuel precursor was obtained over the optimized reaction conditions. The excellent activity can be attributed to the coexistence of HPW, which provides the catalytically active sites, IL groups, which served as anchors of HPW onto the support, and FNS, which improves dispersion of the active sites and accessibility of the reactant molecules through its fibers. The effects of the reaction conditions on the final yield and the carbon balance of the reaction were studied. Furthermore, the catalyst can be effortlessly recovered and reused without appreciable loss of activity. The post reaction characterizations of the spent catalyst show no significant change from the fresh catalyst.

Keywords: Fibrous Silica, Heteropoly Acid, Ionic Liquid, Biomass, Fuel Precursors

INTRODUCTION

As a consequence of the simultaneous growth in the global population and the depletion of our fossil fuel reservoirs, there is a necessity for developing alternative energy sources [1]. Lignocellulosic biomass holds immense potential as a substitute energy source since it is an abundant, renewable, and carbon-neutral feedstock [2]. Inspired by the pioneering works of the groups of Corma [3,4], Dumesic [5,6], and Huber [7,8], a significant amount of research work has been devoted to the catalytic processing of lignocellulosic biomass-derived chemicals to diesel (C9-C22) and jet (C8-C16) fuel range alkanes.

In this context, carbon-carbon coupling reactions, such as hydroxyalkylation-alkylation (HAA), are necessary to upgrade biomass-derived lower carbon molecules to higher carbon fuel precursors [9]. As represented by Scheme 1, HAA requires an acidic catalyst to initiate the electrophilic aromatic substitution that will further produce the diesel and jet fuel range precursors [10]. The HAA of 2-methylfuran (2-MF) and 5-methylfurfural (5-MF) can be considered as a highly efficient C-C coupling reaction since it allows a holistic utilization of lignocellulosic biomass, taking into consideration that 2-MF and 5-MF can be produced from hemicellulose and cellulose, respectively [11,12]. 2-MF is obtained from the selective hydrogenation of furfural [13] while 5-MF is obtained from selective hydrogenolysis of 5-HMF [14].

Though numerous studies have reported HAA reactions, not much research has involved using both 2-MF and 5-MF as starting materials, particularly under heterogeneous acid catalysis. The first report involving the synthesis of C16 fuel precursor from 2-MF and 5-MF employed commercially available homogeneous catalysts such as *para*-toluenesulfonic acid (*p*TsOH) and sulfuric acid (H_2SO_4) [11,13]. After distillation, a 93% and 83% of C16 fuel precursor yield was obtained with *p*TsOH and H_2SO_4, respectively. Although promising results were achieved with these catalysts, tedious product separation and purification steps were needed to obtain the desired product. Moreover, the homogeneity of the reaction environment hindered the recyclability of the catalysts. To the best of our knowledge, the 2011 study by Corma et al is the only study dedicated solely to the reaction of 2-MF and 5-MF. This reaction is otherwise mentioned in other papers as a means to show the applicability of a catalyst system designed for different reaction systems. Thus, no detailed information regarding the optimization of reactant molar ratio to the stoichiometric ratio, effect of reaction condition, effect of catalyst properties, use of heterogeneous catalysts or recyclable of the catalysts used is available. Hence, to overcome the limitations of the existing catalytic systems, there is a necessity for the development of highly active, heterogeneous acid catalysts.

In this context, ionic liquids (ILs) are efficient and active catalysts

†To whom correspondence should be addressed.
E-mail: jgseo@hanyang.ac.kr
‡M. N. Gebresillase and R. Q. Raguindin contributed equally.

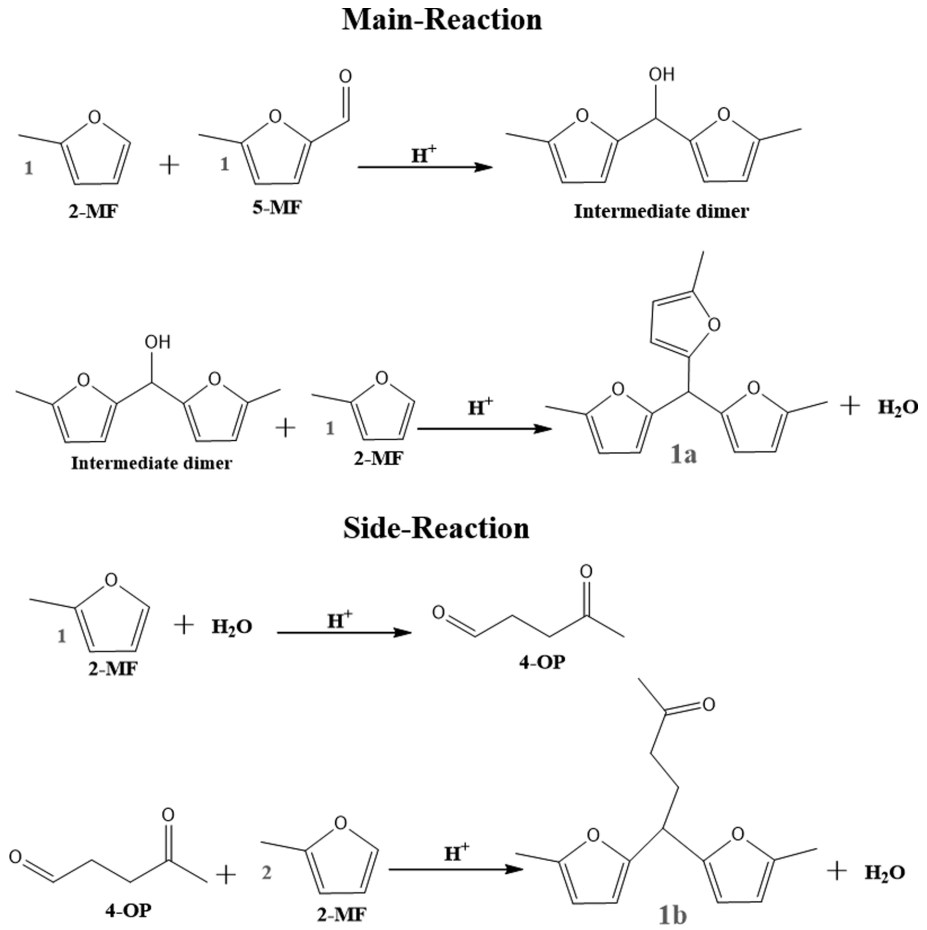

Scheme 1. The reaction pathway for the cross-condensation of 2-methylfuran with 5-methylfurfural.

due to their unique properties such as low volatility, high thermal stability, and outstanding solvation ability for a wide range of materials [14,15]. Although ILs are effective catalysts, their utilization still presents severe drawbacks in downstream processing steps such as their separation, recovery, and reusability. A widely studied approach to overcome these limitations is to immobilize ILs onto a suitable support. The incorporation of support maximizes both homogeneous (high activity) advantages and heterogeneous (ease of separation and reusability) catalysis [16,17]. Fibrous nano-silica (FNS) is considered excellent catalyst support for heteropoly acid-based ionic liquids because of its unique structure, which provides easy accessibility to the reactant molecules through its fibers. Moreover, functional groups can be readily immobilized onto FNS, depending on the requirements of the reaction [18,19].

In this work, we prepared an IL-functionalized fibrous nano-silica material using ionic liquid and tetraethoxysilane as the silica precursors (FNS-IL). This as-synthesized FNS-IL was then used to support the heteropoly acid's immobilization, phosphotungstic acid ($H_2PW_{12}O_{40}$). The prepared fibrous nano-silica (FNS) supported heteropoly acid-functionalized ionic liquid (FNS-ILHPW) was investigated in the solvent-free cross-condensation of 2-MF and 5-MF for the synthesis of C16 fuel precursors. The structure and property of catalysts were investigated through various characterization techniques such as SEM, TEM, BET, XRD, FT-IR, and TGA. Reaction conditions, such as temperature, time, and catalyst loading, were optimized to achieve the maximum yield for C16 fuel precursors. To the best of our knowledge, this is the first study to report the solvent-free cross-condensation of 2-MF and 5-MF over heterogeneous acid catalysts, which provides a yield as high as 95% for C16 fuel precursor. The catalyst exhibits good stability and recyclability since only a negligible loss in its activity was observed after five consecutive reaction runs.

EXPERIMENTAL

1. Materials

The reactants, 2-methylfuran (99%, stabilized) and 5-methylfurfural (99%), were purchased from Sigma-Aldrich, USA. For the synthesis of the catalyst, cetyltrimethylammonium bromide (CTAB) (≥99%), sodium hydride (95% dry), and 1-methylimidazole (99%) were obtained from Alfa Aesar. 3-Chloropropyltriethoxysilane (97$^+$%, nitrogen flushed) and phosphotungstic acid hydrate were procured from Acros Organics, USA. For the quantification and qualification of reaction products, silica gel 60, 0.032-0.063 mm (230-450 mesh) was purchased from Alfa Aesar. All HPLC-grade solvents, such as dichloromethane (≥99%) and methanol (≥99.9%), were acquired from Acros Organics, USA. Tetrahydrofuran (reagent grade), sulfuric acid, and hydrochloric acid (36.5%) were pro-

cured from DaeJung Chemicals, South Korea. The solid acid catalysts, amberlyst-15 (4.7 meq g^{-1}), amberlyst-36, and nafion-212, were obtained from Sigma-Aldrich, USA. The nafion film (thickness: 51 μm) used in this work was cut into about 2×5 mm pieces. All the purchased materials were used without further purification.

2. Methods

2-1. General Procedure for the Preparation of FNS

FNS was synthesized based on a reported procedure with some modifications [21]. In the synthesis of FNS, cetyltrimethylammonium bromide (CTAB 0.75 g, 2 mmol) and urea (0.23 g, 3.8 mmol) were dissolved in deionized water (75 mL). The solution was stirred for 1 h until all the CTAB dissolved. Then a solution of tetraethoxysilane (TEOS, 3.75 g, 18 mmol), cyclohexane (75 mL), and pentanol (5 mL) was added dropwise to the above solution of CTAB and urea in water. The mixture was stirred at room temperature for another hour and transferred into a 200 mL Teflon lined hydrothermal reactor. The reactor was then placed in an oven at 120 °C for 6 h. The mixture was then allowed to cool to room temperature, and the silica was isolated by centrifugation (30 min, 6,000 rpm). After thoroughly washing the isolated solid with deionized water and ethanol, it was dried for 12 h at 40 °C. The as-synthesized silica was calcined at 550 °C with 5 °C ramping for 6 h in air.

2-2. General Procedure for the Preparation of FNS-ILHPW

FNS-ILHPW was synthesized by modifying a previously reported procedure [24]. FNS (1.0 g) was suspended in dry toluene (10 mL) in a 100 ml two-necked round-bottom flask equipped with a reflux condenser and a gas inlet valve for N_2. While being stirred, 3-chloropropyl trimethoxy silane (1.5 g) was added dropwise in 30 minutes. The suspension was refluxed for 48 h. The particles were collected by filtration, washed with ethanol and water, and dried under vacuum 60 °C for 2 h. 1-Methylimidazole (1.8 g) and FNS/3-chloropropyltriethoxysilane were dissolved in anhydrous ethanol (50 mL) under stirring. The resulting mixture was refluxed for 24 h in a 100 ml two-necked round-bottom flask equipped with a reflux condenser and a gas inlet valve for N_2. After the removal of ethanol in a vacuum, the solid was dissolved in water. The obtained solution was concentrated under vacuum and then extracted with ethanol-tetrahydrofuran. Subsequently, ion exchange with $H_3PW_{12}O_{40}$ (100 mmol) in ethanol/water was performed for 60 h at ambient temperature. After the solvent was removed, the resulting mixture was filtered and dried under a vacuum at 100 °C.

2-3. Catalyst Characterization

The BET surface areas of the bare silica and FNS-ILHPW were measured by N_2 adsorption-desorption using a BELSORP-mini II instrument (Bel Japan Inc., Japan) at 77 K. To remove physically adsorbed water and impurities, pre-treatment was conducted at 100 °C for 4 h in a vacuum. The morphology and particle size were studied by field emission scanning electron microscopy (FE-SEM). Images were recorded on a Helios 650 scanning electron microscope and a JEM-2100F (JEOL) microscope equipped with energy-dispersive X-ray (EDX) elemental mapping. Fourier transform infrared (FTIR) spectroscopy, using a Varian 2000 Fourier transforms infrared spectrophotometer, was used to record IR spectra with KBr pellets. The spectrometer was operated in the transmittance mode at a resolution of 4 cm^{-1}. Acid-base titration was used to determine the H^+ ion concentration of the FNS-ILHPW. 150 mg of catalyst was added to the NaCl solution (20 mL, 0.1 M). After the solution was stirred for 24 h, the solid was separated from the solution by filtration. Then the filtrate was titrated to an endpoint at pH of 7 with 0.01 M NaOH. The total acid density of the catalysts was estimated by calculating the amount of NaOH consumed. Thermogravimetric analysis (TGA), using a TGA N 1000 (SCINCO) thermogravimetric analyzer, was used to study the catalysts' thermal stability and degradation patterns. The X-ray diffraction (XRD) patterns were recorded with a 2θ value of 5-80° by D-Max 2500-PC (Rigaku) measurements using Cu-Kα radiation (k=1.541 Å) operated at 50 kV and 150 mA.

2-4. General Procedure for the Condensation Reactions

The cross-condensation reaction of 2-MF and 5-MF was carried out in a 100 mL round bottom flask. In a representative reaction, 2-MF (20 mmol), 5-MF (10 mmol), and catalyst (0.15 g) were mixed at room temperature. The mixture was added to the round bottom flask, which was then connected to a reflux condenser. The reaction temperature was set at 60 °C and controlled using an oil bath. The mixture was refluxed for 2 h. The catalyst was separated by centrifugation and washed with ethanol and water. Before reuse, the catalyst was dried at 80 °C overnight. For the product qualification and quantification, column chromatography was conducted using silica gel and a mixture of dichloromethane and hexane (95 : 5) to separate the products. The obtained products were concentrated by evaporating the solvents. The separated liquid products were analyzed using a high-performance liquid chromatography (HPLC) system equipped with a ZORBAX SB-C18 column (4.6 mm×150 mm×5 μm) and a refractive index detector for identification and quantification. The HPLC settings are column temperature set at 40 °C, binary pump system with a total flow rate of 0.6 ml/min, the cell temperature of the detector set at 35 °C, oven temp (min 40 °C - max 105 °C, sampling speed 5 μl/s and rinse type external only. A mixture of methanol and water (8 : 2) was used as a mobile phase. The conversion of the limiting reactant and yield for the target product were calculated using these equations:

$$\text{Conversion (\%)} = \frac{\text{mols (initial reactant's)} - \text{mols (reactant's at a given time)}}{\text{mols (initial reactant's)}} \times 100\%$$

$$\text{Yield (\%)} = \frac{\text{mols of carbon in the product}}{\text{mols of carbon in the reactant}} \times 100\%$$

RESULTS AND DISCUSSION

FNS-ILHPW was synthesized according to Scheme 2 and was utilized for the cross-condensation reactions. The successful preparation of FNS-ILHPW was evaluated through several characterization techniques.

1. Characterization of the Synthesized Catalysts

The N_2 adsorption-desorption isotherms and pore size distribution of FNS, FNS-ILHPW and RFNS-ILHPW are displayed in Fig. 1. All materials exhibit type-IV isotherms. As expected, a substantial decrease in the textural properties (surface area and pore volume) occurred as shown in Table 1 upon functionalizing FNS, indicating that the preparation method used in this study allowed the IL and HPW groups to be incorporated onto FNS. After five

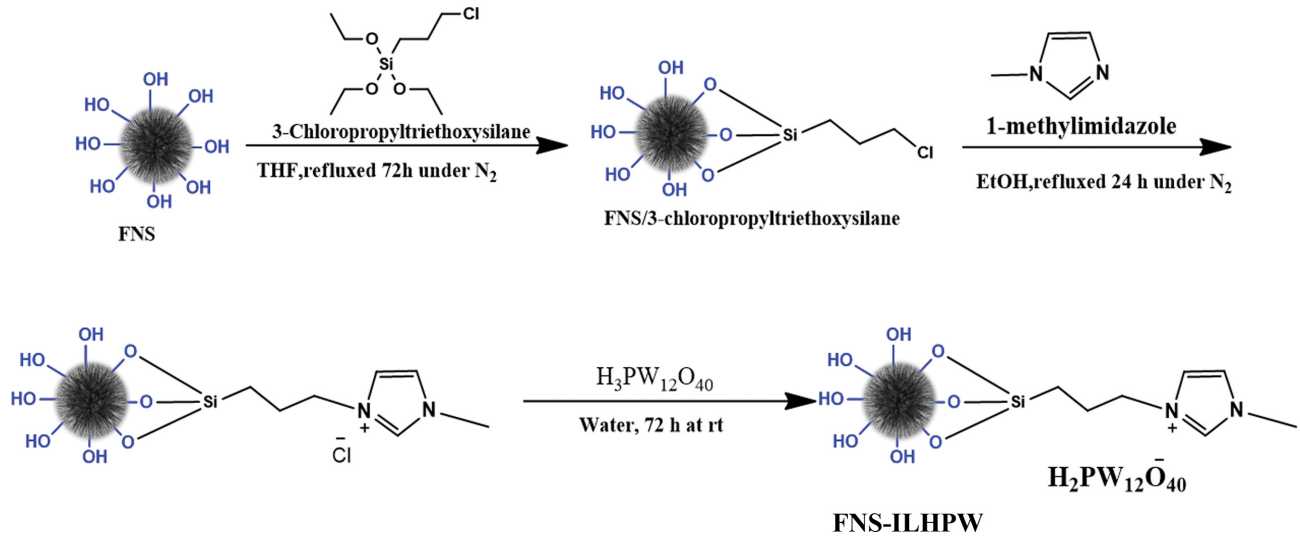

Scheme 2. Schematic representation of the synthesis of FNS-ILHPW.

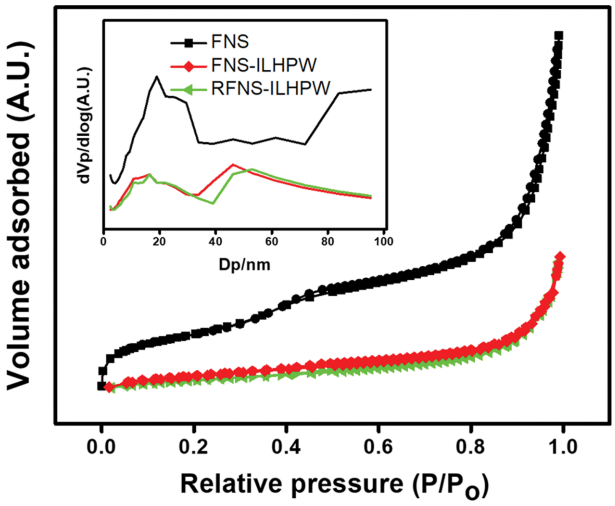

Fig. 1. Adsorption-desorption isotherms and pore size distribution curves (inset) of FNS, FNS-ILHPW and RFNS-ILHPW.

cycles of reactions, FNS-ILHPW was filtered, washed and dried at 80 °C. The sample, RFNS-ILHPW, was then pretreated and set for BET analysis. No significant change in surface area and pore size distribution was observed. The results indicating that the recycled catalyst maintained the textural property even after five cycles [20].

Transmission electron microscopy (TEM) and scanning electron microscopy (SEM) were performed to obtain details of the morphology and structural features of the FNS, FNS-ILHPW and RFNS-ILHPW. The mean diameter of the nanoparticles was found to be 430 nm. Fig. 2(a) displays dendrimeric silica fiber interconnected with each other to form uniform spheres of FNS. From Fig. 2(b), it can be observed that the fibrous morphology of FNS was preserved even after the incorporation of ILHPW. EDS analysis has also confirmed the presence of the elemental components of FNS-ILHPW (Fig. 2(d)-(e)). The SEM and TEM of the recycled sample, RFNS-ILHPW, revealed that the fibrous nature of FNS remained intact after five cycles of reactions (Fig. 2(f)-(h)).

X-ray diffraction (XRD) patterns of FNS, FNS-HPW and FNS-ILHPW were measured to investigate their crystallinity. As shown in Fig. 3, a broad peak between 20-30° attributed to amorphous silica was observed for FNS. No considerable changes were observed with the incorporation of the ionic liquid and heteropolyacid in FNS-ILHPW. Meanwhile the direct incorporation of heteropolyacid to FNS-HPW shows peaks at 20.8°, 33.4°, 38.2°, 41.5°, 49.1°, and 61.7°, that are not present in the spectra of FNS and FNS-ILHPW, which are characteristic of crystalline HPW. The FNS-ILHPW catalyst exhibited a similar pattern with a broad band centered at 23°. Compared with bulk FNS-HPW, which showed various crystalline peaks, no noticeable peaks related to the $H_2PW_{12}O_{40}^-$ were observed in FNS-ILHPW. The obtained result suggests that HPW was present as charge compensating anion ($H_2PW_{12}O_{40}^-$) of

Table 1. Textural property of the FNS, FNS-ILHPW and RFNS-ILHPW

Entry	Catalyst	Specific surface area ($m^2\ g^{-1}$)[a]	Pore volume ($cm^3\ g^{-1}$)[a]	Acidic amount (mmol/g)[b]
1	FNS	500	1.73	0.07
2	FNS-ILHPW	252	0.41	1.37
3	RFNS-ILHPW	245	0.39	1.31

[a]Calculated using Brunauer-Emmett-Teller (BET) method.
[b]Calculated from acid-base titration.

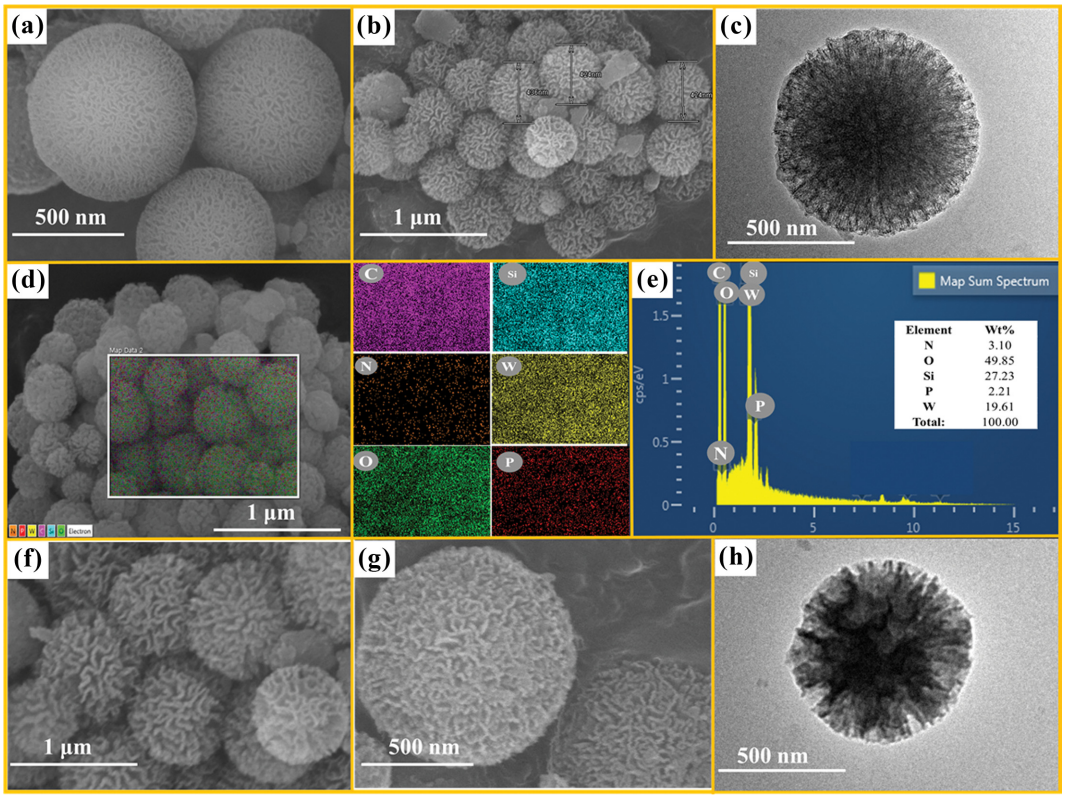

Fig. 2. SEM images of FNS and FNS-ILHPW ((a), (b), (d)), TEM image of FNS-ILHPW (c), Elemental mapping of FNS-ILHPW, EDS spectra of FNS-ILHPW (e), SEM images of RFNS-ILHPW ((f) and (g)) and TEM image of RFNS-ILHPW.

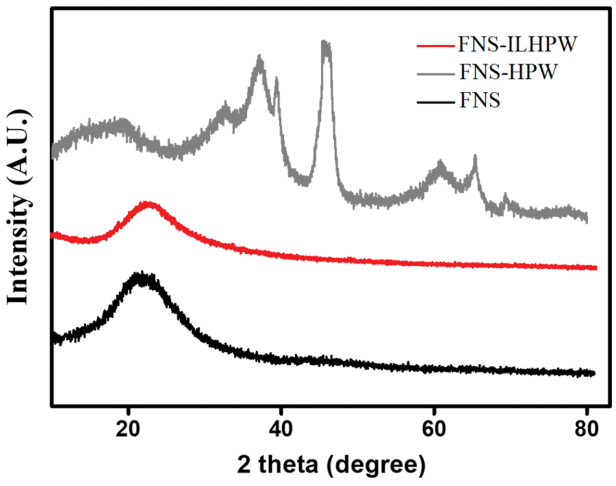

Fig. 3. XRD patterns of FNS, FNS-HPW and FNS-ILHPW.

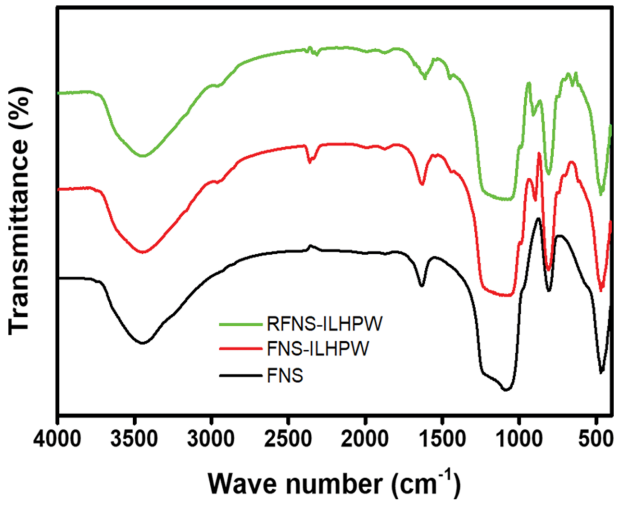

Fig. 4. FTIR spectra of FNS, FNS-ILHPW and RFNS-ILHPW.

the IL and was not in the crystalline form. Both the results from FTIR spectroscopy and XRD are in good agreement with previous studies [21-23].

FTIR spectroscopy was conducted (Fig. 4) to examine the surface modification of FNS after functionalization with ILHPW. Both samples showed the peaks for the symmetric and asymmetric stretching of Si-O-Si bands at 800 and between 1,000-1,250 cm^{-1}. The peaks at 3,016, 2,930 cm^{-1}, and 1,470 cm^{-1} of the FNS-ILHPW spectrum correspond to the stretching vibrations of the C-H bonds of the propyl chain, the vibration of the imidazole ring, and the C=N and aromatic C=C stretching of the imidazolium cation, respectively. These peaks' presence supports the successful immobilization of the imidazolium ionic liquid onto the fibrous nano-silica surface. Also, the characteristic IR bands of HPW (W-O-W) at 890 and 738 cm^{-1} and the peak at 1,090 cm^{-1} attributable to the asymmetric stretching of P-O confirms the incorporation of $H_2PW_{12}O_{40}^-$ into the ionic liquid [18,22,23]. The strong covalent interaction of the functionalized ionic liquid and FNS was further

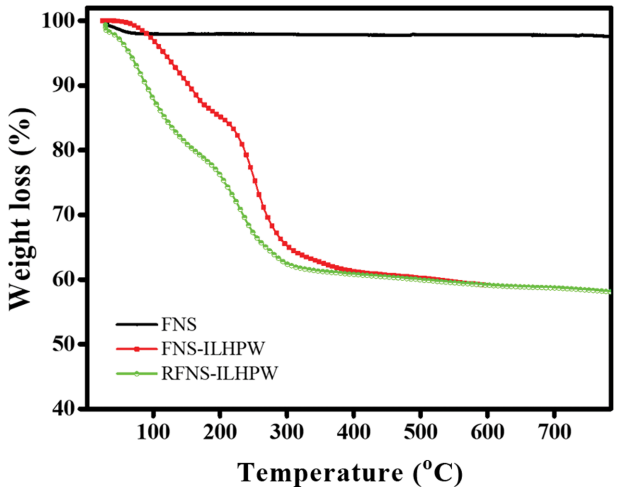

Fig. 5. TGA profiles of FNS, FNS-ILHPW and RFNS-ILHPW.

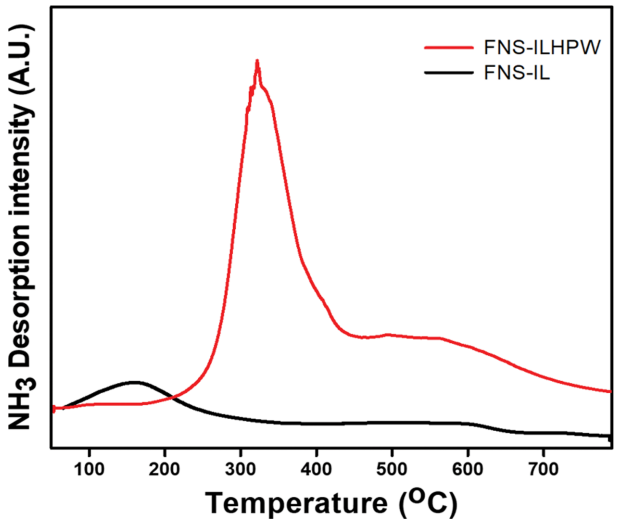

Fig. 6. NH_3-TPD profiles of FNS-IL and FNS-ILHPW.

studied by characterizing the spent catalyst after five times. No alteration was detected in the FTIR spectra of FNS-ILHPW and RFNS-ILHPW, indicating that the IL was indeed covalently bonded with the support thus avoiding leaching.

Thermogravimetric analysis (TGA) was carried out to determine the thermal stability and measure the corresponding content of encapsulated fibrous nano-silica, ionic liquid, and heteropoly acid FNS-ILHPW. As revealed by Fig. 5, three weight loss steps were exhibited by the catalyst for the temperature range of 25-800 °C inflowing air. In the first stage of weight loss (40-150 °C), approximately 15% weight loss was observed, attributed to the physisorbed water. The second weight-loss step of around 25% at 150-300 °C corresponded to the cross-linking organic group derivatives' thermal decomposition [23,24]. The last weight loss of about 5% at 300-500 °C is ascribed to the pyrolysis of HPW and its related ammonium salts. The degradation patterns of RFNS-ILHPW and FNS-ILHPW, show a slight difference between the first and the second stage of weight-loss. The increase in the weight-loss for RFNS-ILHPW in the first stage (40-150 °C) can be attributed to the physisorbed water and residual reactants after washing. The second increase in weight-loss can be attributed to the degradation of the residual polymeric product after watching. Interestingly, there was no significant increase in the last stage of degradation (300-500 °C), which was ascribed to the pyrolysis of HPW and its related ammonium salts, indicating that there was no major change in the initial HPA loading after five cycles. The result was in agreement with the values obtained from the titration.

NH_3-TPD analysis was used to study the catalysts before and after the integration of HPW anion to investigate the effect in the acidic strength of the catalysts. Fig. 6 shows the NH_3-TPD analysis of the FNS-IL and FNS-ILHPW, respectively. The acid sites were identified and categorized based on desorption temperature. The temperature in the range 25-200 °C corresponds to weak acid since chemisorbed ammonia with weak interactions is desorbed at low temperatures. Meanwhile, the ammonia desorption temperature 200-400 °C and above 400 °C indicates medium and strong acid sites. The desorption profile of FNS-IL consists of one minor peak at low temperatures (50-270 °C), which is assigned to weak acid sites. However, the desorption peak of FNS-ILHPW shows two peaks at higher temperature than FNS-IL. The broad peak in the temperature between 250-450 °C corresponds to moderately strong acid sites while the smaller high temperature desorption peak is attributed to stronger acid sites [22].

2. Catalytic Activity of FNS-ILHPW

The cross-condensation of 2-MF and 5-MF was investigated over the commercially available homogeneous and heterogeneous catalysts. 1a was identified as the primary product from HPLC and NMR (Figs. S1-S3). The performance of the catalysts decreased in the order of FNS-ILHPW≈*p*TsOH (95% C16 yield)>HPW (83%)>Nafion-212 (80%)>Amberlyst-15 (73%) as shown on Fig. 7. A high yield of 95% for C16 fuel precursor was reached under the catalysis of FNS-ILHPW. Although *p*TsOH and unsupported heteropoly acid (HPW) is an effective catalyst for this reaction, the recovery and reusability challenges remain significant. Meanwhile, the higher performance with excellent recovery and reuse was obtained by grafting HPW onto appropriate support.

The performance of commercial resins, Nafion-212 and Am-

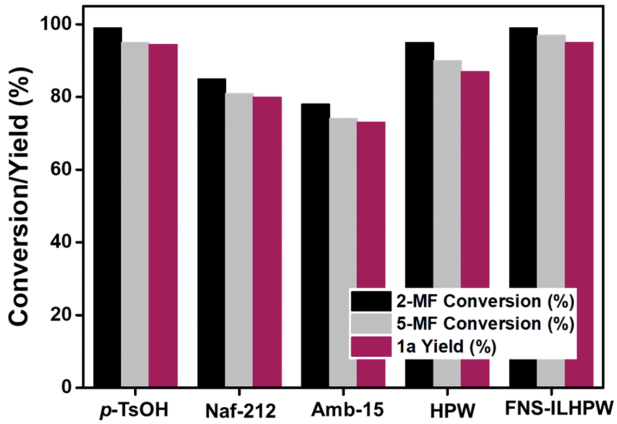

Fig. 7. Catalyst comparison for the HAA of 2-MF with 5-MF. Reaction conditions: 40 mmol 2-MF, 20 mmol 5-MF, 5 wt% catalyst (heterogeneous), 60 °C, 2 h.

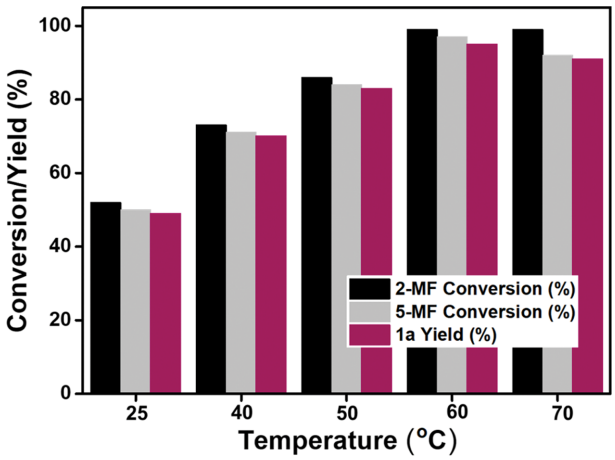

Fig. 8. Influence of reaction temperature. Reaction conditions: 40 mmol 2-MF, 20 mmol 5-MF, 5 wt% catalyst, 2 h.

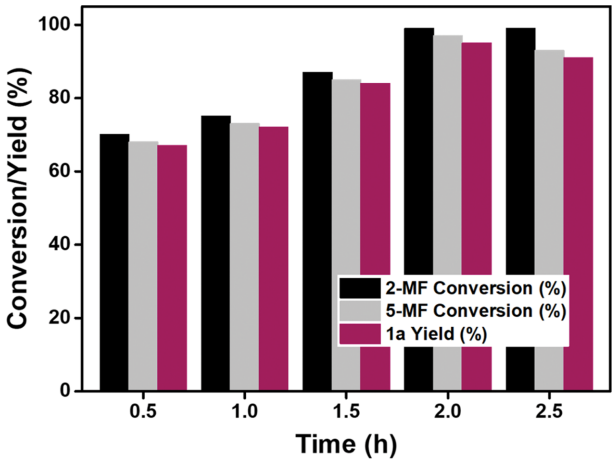

Fig. 9. Influence of reaction time. Reaction conditions: 40 mmol 2-MF, 20 mmol 5-MF, 5 wt% catalyst, 60 °C.

berlyst-15, was also studied, and both provided a significant yield for C16 trimer. Nafion-212 is a perfluorinated sulfonic acid resin; hence, the SO_3H groups' acidic strength is enhanced by the presence of fluorine. On the other hand, Amberlyst-15 is a sulfonic acid functionalized cross-linked polystyrene with increased surface wettability. The by-product of the reaction 1b (5,5-bis(5-methyl-2-furanyl)-2-pentanone) Scheme 1, was formed significantly when Amberlyst-15 was used as a catalyst. This can be explained by the self-condensation of 2-MF is the hydrolysis (ring-opening) reaction of 2-MF in the presence of in situ produced H_2O to synthesize the intermediate aldehyde 4-oxopentanal (4-OP) due to the hydrophilic nature of Amberlyst-15. The intermediate aldehyde then underwent alkylation with the remaining two moles of 2-MF to form the C15 trimer 1b [21]. The excellent catalytic performance exhibited by FNS-ILHPW is associated with the collaborative efforts of HPW, which provided the catalytically active sites, IL groups, which served as anchors of HPW onto the support and increases solubility, and the fibrous nature, which improved dispersion of the active sites and better accessibility of the reactant molecules through its fibers.

The reaction conditions (temperature, time, and catalyst loading) were optimized (Figs. 8-10) to achieve the maximum C16 yield. FNS-ILHPW was active even at room temperature, giving 53% 2-MF conversion and 47% C16 trimer yield. Raising the temperature to 60 °C remarkably increased both the conversion of the reactants and the C16 trimers (Fig. 8). A yield of 95% was achieved at 60 °C. While the conversion slightly increased with increasing the temperature to 70 °C, the yield for C16 decreased to 91%; thus, it did not significantly improve the catalytic activity. Hence, 60 °C was the optimum reaction temperature for the cross-condensation of 2-MF and 5-MF.

Prolonging the reaction time enhanced the yield for C16 fuel precursor from 64% at 0.5 h to 95% at 2 h of reaction (Fig. 9). Further extending the time for another 30 minutes did not substantially improve the catalytic activity. Hence, all the succeeding experiments were completed for 2 h. Further increasing reaction time may push the reaction towards the formation of oligomers and polymers.

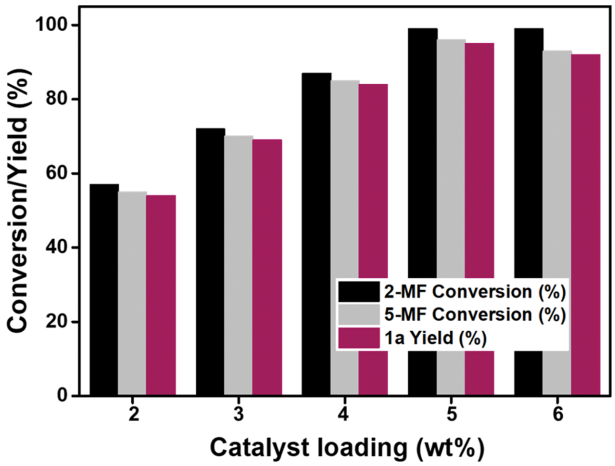

Fig. 10. Influence of catalyst loading. Reaction conditions: 40 mmol 2-MF, 20 mmol 5-MF, 60 °C, 2 h.

For the last part of the optimization of reaction conditions, the influence of catalyst loading was studied. The effect of catalyst amount on reactant conversion and C16 yield was studied for the optimum temperature and time. Fig. 10 shows the C16 yield and with 2-MF and 5-MF conversion by varying the quantity of FNS-ILHPW. It can be deduced that an increase in the dosage of the catalyst led to an enhancement of the activity, providing 53% yield at 2 wt% and 95% at 5 wt% loading. This improvement is due to the higher concentration of the available active sites at higher catalyst loading. Further increase in FNS-ILHPW slightly decreased the C16 yield, which can be attributed to the formation of polymeric compounds due to increased acidity in the system.

The effect of the reaction conditions was further analyzed by calculating the overall carbon balance provided on Table S1. At lower temperature, time, and loading, the reaction mixture contains a significant amount of C5 and C6 from the unreacted 2-MF and 5-MF. The overall carbon balance at these conditions indicates that almost all the carbon fed is accounted for in the liquid phase. However, at higher temperature, prolonged time and increased catalyst

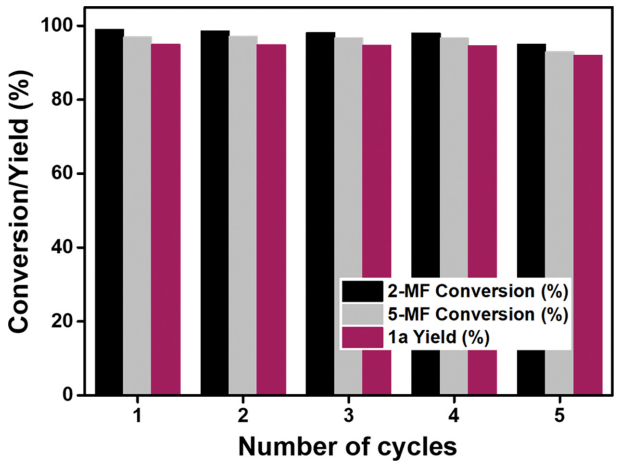

Fig. 11. Recyclability tests. Reaction conditions: 40 mmol 2-MF, 20 mmol 5-MF, 5 wt% catalyst, 60 °C, 2 h.

loading, by-products like self-trimer of 2-MF are observed and the overall carbon balances are ~97%. With increase in the reaction conditions, the tetramer of 2-MF and some carbon deposition was observed on the catalyst surface and reaction mixture indicative of oligomerization with the increase in temperature and time. Although not shown on the manuscript, we conducted the reaction at 80 and 90 °C, which led to severe polymerization [1,3,21].

Although catalytic activity and selectivity are important for developing a process that can compete with the existing petrochemical processes, catalyst stability must also be guaranteed for long-term operation to increase the cost efficiency [25]. Thus, the recyclability and stability of FNS-ILHPW were evaluated by conducting five successive reaction runs. After the reaction, the catalyst was filtered, washed with ethanol, dried in a vacuum at 60 °C for 6 h, and reused for the next run. The normalized values of conversion and yield, accounting for the loss of catalyst during recovery, are shown in Fig. 11, demonstrating that FNS-ILHPW can be reused for five consecutive reactions without a considerable loss in its activity. Catalyst stability can be credited to the IL groups grafted onto FNS, which served as robust anchors that prevented heteropoly acid leaching.

CONCLUSIONS

A fibrous nano-silica supported heteropolyacid-based ionic liquid, FNS-ILHPW, was successfully synthesized and applied in the cross-condensation of lignocellulosic biomass-derived 2-MF and 5-MF to produce higher carbon fuel precursors. The characterization results showed the unique fibrous morphology of the silica support, the accessibility of the active, high surface area and high pore volume, and the advantages of the IL in terms of solubility in the development of efficient catalysts. The XRD and FTIR indicate that HPW was present as charge compensating anion ($H_2PW_{12}O_{40}^-$) of the IL, while NH_3-TPD analysis revealed that the integration of HPW resulted in moderate to strong acid sites. Excellent conversion of the starting materials and yield for C16 trimer (1a, 2, 2′,2″-methylidenetris[5-methylfuran]) was obtained over FNS-ILHPW. With the optimized reaction conditions, a yield of 95% for C16 fuel precursor was achieved. The by-product of the reaction is 1b (5,5-bis(5-methyl-2-furanyl)-2-pentanone), which is the result of the self-condensation of 2-MF from the hydrolysis (ring-opening) reaction of 2-MF in the presence of in situ formed H_2O. The effect of the reaction conditions was further analyzed by calculating the overall carbon balance. Lower temperature, time, and loading, the reaction mixture contains a significant amount of C5 and C6 from the unreacted 2-MF and 5-MF. With increase in the reaction conditions, the tetramer of 2-MF and some carbon deposition was observed on the catalyst surface and reaction mixture. After five reaction cycles, no significant textural and structural property change was observed for the recycled catalyst. The utilization of lignocellulosic biomass-derived 2-MF together with 5-MF in the synthesis of fuel precursor here allows the consumption of both the hemicellulosic and cellulosic portions of biomass.

ACKNOWLEDGEMENTS

This work was supported by the Energy Efficiency & Resources Program (No. 20183030092080) of the Korea Institute of Energy Technology Evaluation and Planning (KETEP) grant funded by the Korea government Ministry of Trade, Industry & Energy. This work was also supported by the National Research Foundation of Korea (NRF) grant funded by the Korea government (MSIT) (No. 2020R1A5A1019131).

CONFLICTS OF INTEREST

There are no conflicts of interest to declare.

SUPPORTING INFORMATION

Additional information as noted in the text. This information is available via the Internet at http://www.springer.com/chemistry/journal/11814.

REFERENCES

1. D. M. Alonso, J. Q. Bond and J. A. Dumesic, *Green Chem.*, **12**, 1493 (2010).
2. F. H. Isikgor and C. R. Becer, *Polym. Chem.*, **6**, 4497 (2015).
3. A. Corma, O. De La Torre, M. Renz and N. Villandier, *Angew. Chem. - Int. Ed.*, **50**, 2375 (2011).
4. A. Corma, O. De Torre and M. Renz, *ChemSusChem*, **4**, 1574 (2011).
5. J. C. Serrano-ruiz and J. A. Dumesic, *Green Chem.*, **11**, 1101 (2009).
6. J. C. Serrano-ruiz and J. A. Dumesic, *Energy Environ. Sci.*, **4**, 83 (2009).
7. H. Olcay, A. V. Subrahmanyam, R. Xing, J. Lajoie, J. A. Dumesic and G. W. Huber, *Energy Environ. Sci.*, **6**, 205 (2013).
8. J. Q. Bond, A. A. Upadhye, H. Olcay, G. A. Tompsett, J. Jae, R. Xing, D. M. Alonso, D. Wang, T. Zhang, R. Kumar, A. Foster, S. M. Sen, C. T. Maravelias, R. Malina, S. R. H. Barrett, R. Lobo, C. E. Wyman, J. A. Dumesic and G. W. Huber, *Energy Environ. Sci.*, **7**, 1500 (2014).

9. H. Li, A. Riisager, S. Saravanamurugan, A. Pandey, R. S. Sangwan, S. Yang and R. Luque, *ACS Catal.*, **8**, 148 (2018).
10. G. Li, N. Li, G. Li, L. Li, A. Wang, Y. Cong, X. Wang and T. Zhang, *ChemSusChem*, **5**, 1958 (2012).
11. A. Corma, O. De Torre and M. Renz, *ChemSusChem*, **4**, 1574 (2011).
12. W. Yang and A. Sen, *ChemSusChem*, **4**, 349 (2011).
13. S. Sadjadi, V. Farzaneh, S. Shirvani and M. Ghashghaee, *Korean J. Chem. Eng.*, **34**, 692 (2017).
14. C. Xiong, Y. Sun, J. Du, W. Chen, Z. Si, H. Gao, X. Tang and X. Zeng, *Korean J. Chem. Eng.*, **35**, 1312 (2018).
15. A. Corma, O. De Torre and M. Renz, *Energy Environ. Sci.*, **5**, 6328 (2012).
16. O. Bartlewicz, I. Dabek, A. Szymanska and H. Maciejewski, *Catalysts*, **10**, 1227 (2020).
17. Q. Zhang, S. Zhang and Y. Deng, *Green Chem.*, **13**, 2619 (2011).
18. K. B. Sidhpuria, A. L. Daniel-Da-silva, T. Trindade and J. A. P. Coutinho, *Green Chem.*, **2**, 340 (2011).
19. H. Li, S. Saravanamurugan, S. Yang and A. Riisager, *ACS Sustain. Chem. Eng.*, **3**, 3274 (2015).
20. V. Polshettiwar, D. Cha, X. Zhang and J. M. Basset, *Angew. Chem. - Int. Ed.*, **49**, 9652 (2010).
21. M. N. Gebresillase, R. Shavi and J. G. Seo, *Green Chem.*, **20**, 5133 (2018).
22. P. Sudhakar and A. Pandurangan, *Mater. Renew. Sustain. Energy*, **8**, 22 (2019).
23. S. M. Sadeghzadeh, *RSC Adv.*, **6**, 75973 (2016).
24. S. M. Sadeghzadeh, *Green Chem.*, **17**, 3059 (2015).
25. S. Kim, Y. F. Tsang, E. E. Kwon, K. Y. A. Lin and J. Lee, *Korean J. Chem. Eng.*, **36**, 1 (2019).

Supporting Information

Application of 2-methylfuran and 5-methylfurfural for the synthesis of C16 fuel precursor over fibrous silica-supported heteropoly acid-functionalized ionic liquid

Mahlet Nigus Gebresillase*,‡, Reibelle Quiambao Raguindin,‡, and Jeong Gil Seo*,†**

*Department of Chemical Engineering, Hanyang University, 222 Wangsimni-ro, Seongdong-gu, Seoul 04763, Korea
**Department of Energy Science and Technology, Myongji University,
116 Myongji-ro, Cheoin-gu, Yongin-si, Gyeonggi-do 17058, Korea
(*Received 14 November 2020 • Revised 15 February 2021 • Accepted 23 February 2021*)

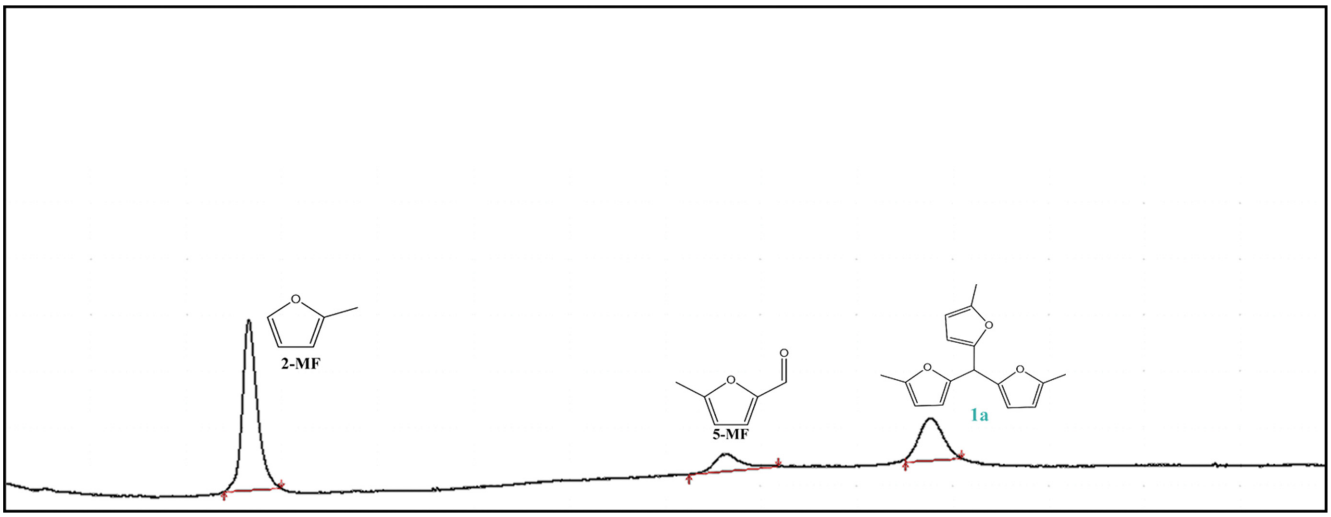

Fig. S1. HPLC chromatogram of the reaction mixture from the cross-condensation of 2-MF and 5-MF. Reaction conditions: 40 mmol 2-MF, 20 mmol 5-MF, 60 °C, 2 h, 5 wt% FNS-ILHPW.

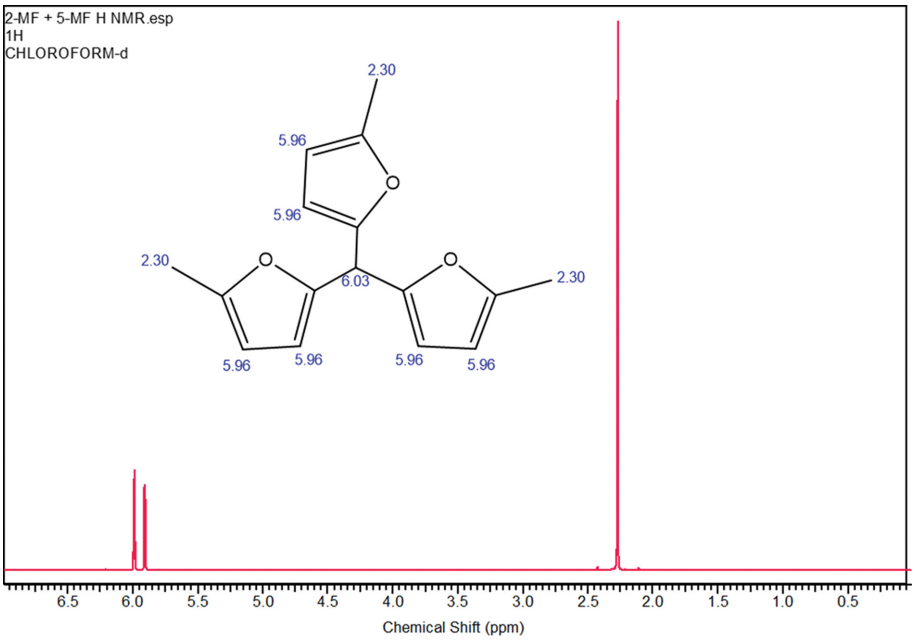

Fig. S2. ^{1}H NMR spectra of the 1a produced from the cross-condensation of 2-MF and 5-MF.

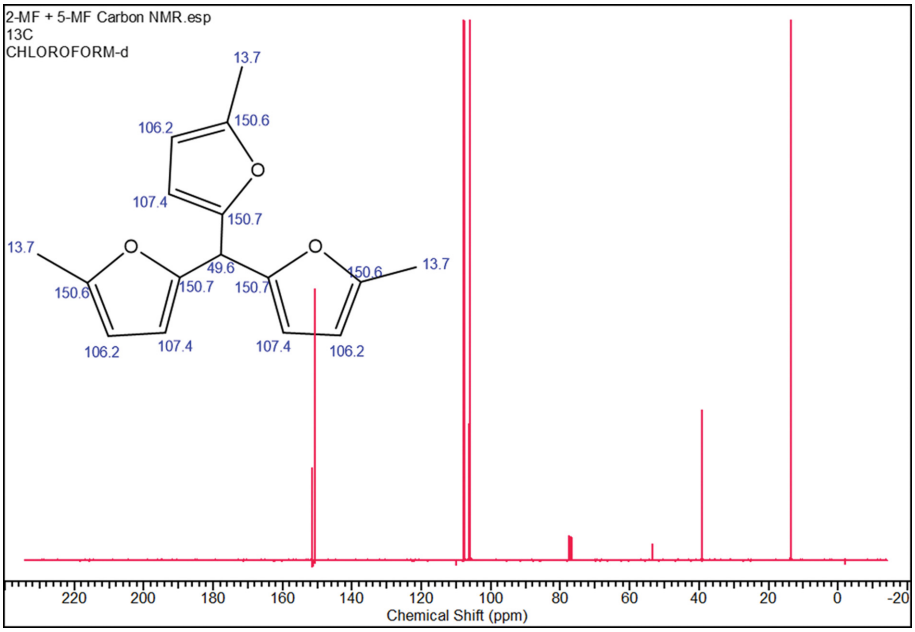

Fig. S3. ^{13}C NMR spectra of the 1a produced from the cross-condensation of 2-MF and 5-MF.

Carbon balance over FNS-ILHPW

$$\text{Overall Carbon balance of liquid products (\%)} = \frac{\text{Sum of carbon in the all liquid hydrocarbons detected from the liquid phase product}}{\text{Carbon fed in the reaction}} \times 100\%$$

Table S1. Overall carbon balance for the different reaction parameters

Entry	Reaction condition	C5-C6	C16	C15	Overall carbon balance (%)
1	40 mmol 2-MF, 20 mmol 5-MF, 5 wt% catalyst, 2 h at 25 °C	32.0	67.1	0.7	99.8
2	40 mmol 2-MF, 20 mmol 5-MF, 5 wt% catalyst, 2 h at 40 °C	25.9	72.3	1.3	99.5
3	40 mmol 2-MF, 20 mmol 5-MF, 5 wt% catalyst, 2 h at 50 °C	13.6	84.4	1.7	99.7
4	40 mmol 2-MF, 20 mmol 5-MF, 5 wt% catalyst, 2 h at 60 °C	1.7	95.2	2.2	99.1
5	40 mmol 2-MF, 20 mmol 5-MF, 5 wt% catalyst, 2 h at 70 °C	2.1	91.3	3.8	97.2
6	40 mmol 2-MF, 20 mmol 5-MF, 5 wt% catalyst, at 60 °C for 30 min	50.0	49.3	0.6	99.9
7	40 mmol 2-MF, 20 mmol 5-MF, 5 wt% catalyst, at 60 °C for 60 min	28.7	70.1	0.9	99.7
8	40 mmol 2-MF, 20 mmol 5-MF, 5 wt% catalyst, at 60 °C for 90 min	14.9	83.0	1.6	99.5
9	40 mmol 2-MF, 20 mmol 5-MF, 5 wt% catalyst, at 60 °C for 120 min	1.7	95.2	2.2	99.1
10	40 mmol 2-MF, 20 mmol 5-MF, 5 wt% catalyst, at 60 °C for 150 min	2.3	91.3	3.3	96.9
11	40 mmol 2-MF, 20 mmol 5-MF, 2 wt% catalyst, 2 h at 40 °C.	44.7	54.5	0.4	99.6
12	40 mmol 2-MF, 20 mmol 5-MF, 3 wt% catalyst, 2 h at 40 °C.	29.9	69.3	0.6	99.8
13	40 mmol 2-MF, 20 mmol 5-MF, 4 wt% catalyst, 2 h at 40 °C.	13.9	84.2	1.6	99.7
14	40 mmol 2-MF, 20 mmol 5-MF, 5 wt% catalyst, 2 h at 40 °C.	1.7	95.2	2.2	99.1
15	40 mmol 2-MF, 20 mmol 5-MF, 6 wt% catalyst, 2 h at 40 °C.	2.0	93.1	3.0	98.1